

Successful early warning and emergency response of a disastrous rockslide in Guizhou province, China

Abstract Early warning of landslides is crucial for risk management and reduction, attracting a lot of attention from both scientists and stakeholders. However, it is challenging due to the complex nature of landslide behaviors and failure mechanisms. Here, we present a recent case of successful early warning and timely evacuation in advance of a large rockslide that occurred on 17 February 2019, in Guizhou Province, China. The rockslide was initially triggered in 2014 due to the excavation of slope toe for road expansion. Since then, the rockslide had become a potential threat to the local residents, pedestrians, and traffic. To ensure their safety, a wireless monitoring network combining on-site sensors and the geodetic method by Global Navigation Satellite System (GNSS) was installed to continuously monitor the surface displacement of the rockslide. Field monitoring data measured by crack gauges, rain gauges, and tiltmeter were transmitted to a real-time early warning system developed using the new artificial intelligence by the authors' institute. Since the deformation of the rock mass was found increasing, nearby residents were evacuated immediately. Using predefined early warning thresholds for rockslides in the system, the rockslide was successfully forecasted 53 min in advance. Prompt action taken by scientists and local authorities averted human and economic losses completely. In this study, we introduce the real-time early warning system, its concept, the method for determining warning threshold, and performance, followed by the emergency mitigation measures performed for this particular rockslide. It is the 5th time our early warning system successfully forecasted a landslide since its implementation in 2017, and hence we discuss the key characteristics of the system in order to make it applicable for other cases globally.

Keywords Landslide early warning · Monitoring · Emergency response · Mitigation measures

Introduction

On 17 February 2019, a large rockslide occurred in Longjing village, Xingyi city, Guizhou province, China. The rockslide was initially triggered in 2014 due to the removal of rock mass near the slope toe for road construction. After the initial event, destabilized loose rock masses and residual rock deposits with an estimated volume of 1.4 million m³ were identified potentially unstable, directly threatening the safety of more than 400 residents, pedestrians, and traffic in the near vicinity. To avert human and economic losses, emergency mitigation measures were implemented and a self-developed real-time landslide early warning system (LEWS) of the State Key Laboratory of Geohazard Prevention and Geoenvironment Protection (SKLGP) (Xu et al. 2009, 2011; Ju et al. 2015; Fan et al. 2019) was deployed over potentially unstable rock masses. Once found the deformation was increasing critically, nearby residents were evacuated weeks before the actual rockslide. A successful prediction of the rockslide was achieved 53 min before the occurrence on 17 February 2019. No injuries, casualties, and

property losses were reported. The key to this successful LEWS lies in: (1) the understanding of local geology and deformation history, (2) the ability to pre-identify and measure indicators of slope deformation, (3) the preciseness of the early warning model for issuing alert levels, (4) immediate action to evacuate local residents, (5) and most importantly the responsible collaboration between local authorities and scientists.

Prediction of landslides is a global challenge for geoscientists due to the complex nature of landslide failure mechanisms (Fukuzono 1990; Crosta and Agliardi 2003; Ju et al. 2015; Loew et al. 2016; Intrieri et al. 2019). Catastrophic landslides often occur suddenly without any noticeable precursors, and some even without any triggers, i.e., the slow-moving gravitational landslides (Fukuzono 1990; Popescu and Sasahara 2009; Gariano and Guzzetti 2016; Pecoraro et al. 2018). To overcome these challenges, we have studied and monitored more than hundreds of multiple types of landslides (rockslides, soil slides, shallow slope failures, etc.) in Southwest China, collecting data from cases involving varied geological formations and climatic contexts, since the inception of our LEWS. Based on the monitoring data from a large number of landslides, we found that most of the landslides that were considered sudden failures actually underwent a deformation process. The difference is that some landslides have longer deformation period before failure (years, months, and days) than some others (hours, minutes). With this know-how, a real-time early warning system based on the new artificial intelligence and data transmission technologies was developed by SKLGP. This system has successfully predicted five landslides since 2017 and saved thousands of lives in China (see Fig. 1).

The deformation of the Longjing rockslide started to increase severely in June 2018, confirmed by visual observation of continuous development of many cracks. The emergency prevention measures by assembling sandbags and installing pile reinforcements in front of the rockslide toe (see Sect. [Early warning and emergency mitigation measures](#) for the chronology of mitigation measures) were also implemented. Meanwhile, the field monitoring network was installed by SKLGP on 27 January 2019. Monitoring devices, i.e., crack gauges, etc. was set up over potentially unstable zones (see Sect. [Monitoring strategies](#) for further details). These crack gauges can adjust the sampling frequency according to the displacement rate of landslides ensuring full control over the landslide deformation. Continuous measurement of displacements from the crack gauges was received and processed in real-time by the server system of the LEWS (situated in the office of SKLGP) which time to time checked the threshold levels and sent warning messages to cellphones of the experts which can be viewed through an Android APP.

At 5:00 a.m., 17 February 2019, the LEWS team was forewarned by the critical warning messages. In an immediate response to the emergency, our team quickly checked the monitoring data and confirmed that the deformation was rapidly increasing and marching into the final stage of an accelerated slope deformation,

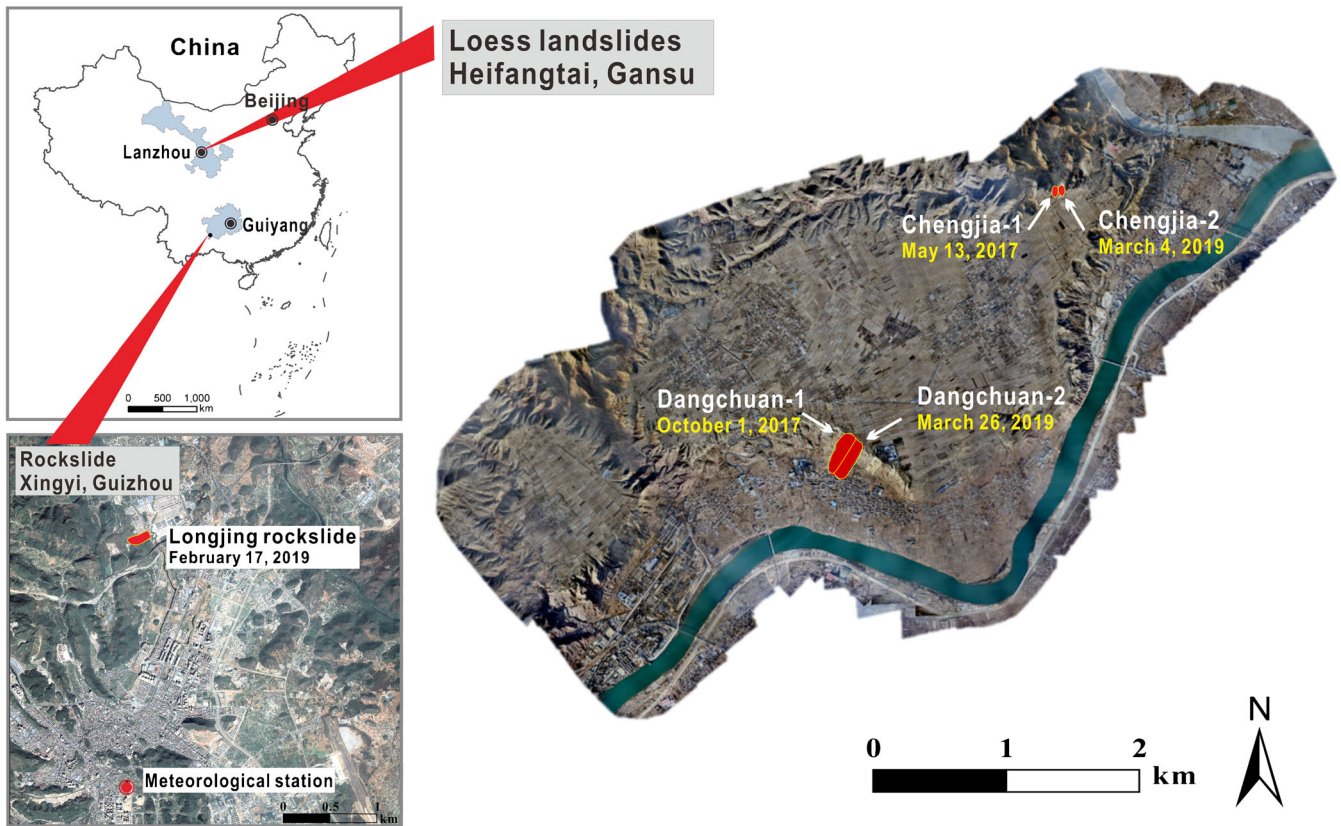


Fig. 1 Map showing locations in China where SKLGP's early warning system successfully predicted the landslides (see Table 2 for details)

which indicated the forthcoming rockslide. Immediately after this, the information was sent out to the local government and then to the public. Owing to the preplanned mitigation measures and early evacuation of all the field personnel and nearby residents, damages from the catastrophe was completely averted. In this study, the application of our self-developed LEWS to the Longjing rockslide is described, covering the aspects of geological setting, deformation history, monitoring strategies, early warning model, and corresponding emergency mitigation measures. This case provides an impressive example of how a LEWS can help during an emergency response for preventing and mitigating landslide risks. In addition, we review the cases of landslides which were predicted successfully by our LEWS and explain some key characteristics of the model which have played a major role in pre-determining the oncoming disaster. We believe the practical implementations and the successful history of our LEWS will surely benefit other countries as well and improve global landslide resiliency.

Background

Geological setting

The rockslide is located in Longjing village, Maling town, 7 km far from Xinyi city of Guizhou province in Southwest China ($104^{\circ} 54' 12''$ N and $25^{\circ} 09' 25''$ E). The locations of the recent rockslide and other four successful early warning of loess landslides are shown in Fig. 1.

The study area is predominantly covered by karst landforms with strong records of incision and erosion processes (Huang et al.

2012a; Guo et al. 2013). A detailed geological investigation and drilling was performed to identify the lithology. The strata outcrops belong to Yangliu (T_2y) formation, Guanling (T_2gl) formation and Jialingjiang (T_{1-2j}) formation of Middle Triassic and Quaternary periods (Fig. 2). The upper parts of the hill slope are 50° to 70° steeper while the lower parts having a slope angle of 15° to 28° . The climate is classified as subtropical monsoon climate, with an average annual temperature ranging between 14 and 19 $^{\circ}$ C and average annual precipitation between 1300 and 1600 mm. The major rainfall concentrates during May to October, and the maximum daily rainfall recorded over the years was 203 mm on 27 August 2015. The above-mentioned temperature and rainfall statistics were obtained from a meteorological station ($104^{\circ} 54' 03''$ N, $25^{\circ} 05' 06''$ E) in Xingyi city located 7.4 km far from the rockslide (see Fig. 1 for location).

The sliding area is conditioned by one fault (F_3) and two suspected faults (F_1 and F_2). F_2 is one of the significant discontinuity structures controlling the slope deformation along the back scarp in the NW-SE direction. The F_3 dipping $290^{\circ} \angle 60^{\circ}$ accompanied with F_2 forms the potentially unstable area which is susceptible for sliding, having an estimated volume of 6 million m^3 . Zone I (marked as I in Fig. 2), the highly deformed area under compression of the upper rock mass, together with Zone II (marked as II in Fig. 2) are further considered potentially unstable areas. A cross-section of the rockslide is taken along 1-1' line and shown in Fig. 3.

As illustrated in Fig. 3, the rockslide body mainly consists of gray-white-colored thick and layered dolomite, a hard competent

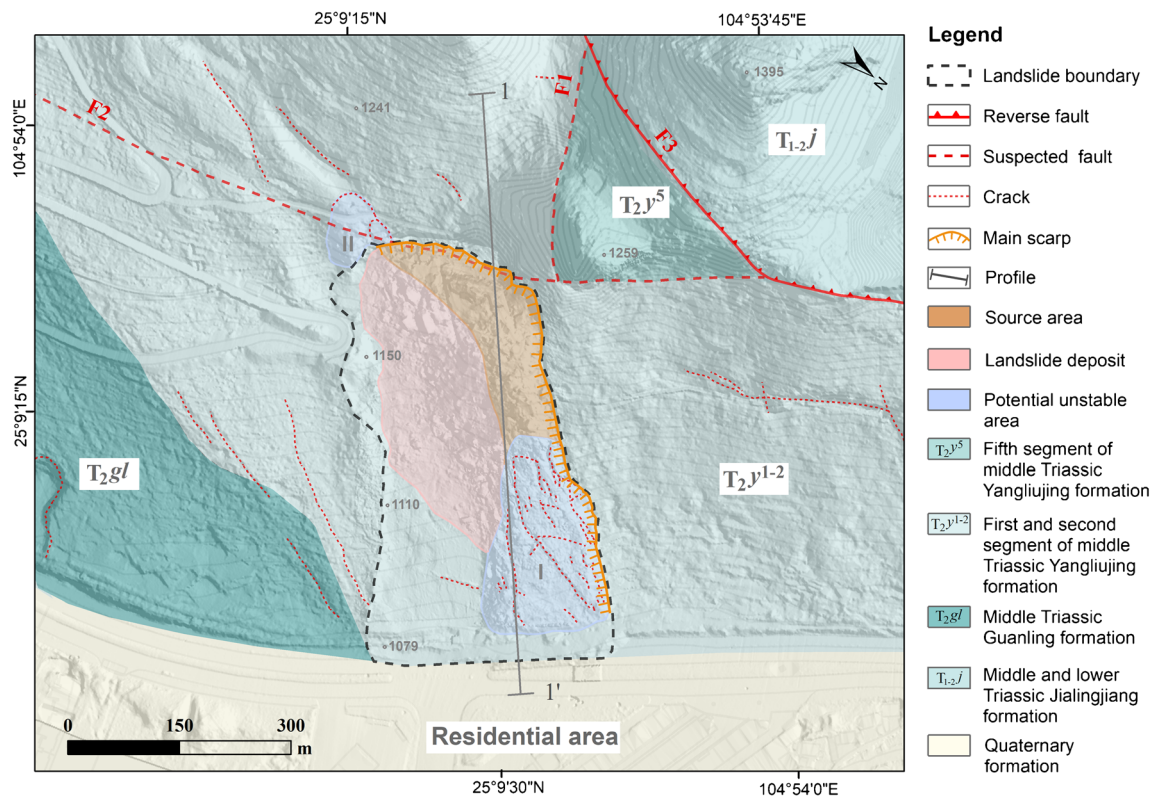


Fig. 2 Geological map of the study area

rock mass, which slid along a weak layer of bedrock mostly consisting of argillaceous limestone and argillaceous dolomite (see the inset in Fig. 3 for enlarged view showing argillaceous limestone, argillaceous dolomite, and weak interlayer) with an estimated volume of 1.4 million m³. In between the dolomitic rock layers, a 2–5-cm-thick interlayer of clay is found along the front edge of the rockslide. The relative height difference between the peak of the rockslide scar and the road at the foot of the slope is around 252 m. The weak clay interlayers might have made the rock mass prone to sliding under a gravitational effect. From this longitudinal profile (Fig. 3), it was confirmed that the ~40–50-m-tall dolomite block sitting at the uphill with a ~45° slope angle will no longer be stable without additional reinforcements at the slope toe. Considering these aspects, pile reinforcements were constructed and temporal sandbags were stacked at the slope toe, which helped to reduce the impact and travel distance during the 17 February 2019 rockslide (see Sect. [Early warning and emergency mitigation measures](#) for details).

Deformation history

The deformation history of the rockslide was analyzed using multi-temporal images obtained from Google Earth since February 2014. The results demonstrate how the discontinuities of the rock mass, i.e., cracks were widened and developed under the influence of anthropogenic activities (Fig. 4a–f). In 2014, there was road construction and expansion of the existing road. The rock mass at the toe of the slope (Fig. 4a) has been excavated, which eventually exposed a major discontinuity (main scarp in orange). The major discontinuity/opening seen in Fig. 4a suggests that the slope had

undergone long-term deformation. Once the road construction started, the deformation was accelerated due to further removal of rock mass from the foot of the slope, followed by a small-scale bedding failure (Fig. 4b). Here, we can assume that the potential zones marked in yellow (Fig. 4a) should have failed along with additional rock mass. Since we lack images immediately after the collapse, it was not possible to delineate the actual extent of the first occurrence of this rockslide. In 2016, the collapsed rock masses have been completely removed (clear bedrock as shown in Fig. 4c) to avoid further movement of deposits by rainfall. The upper part of the sliding body consists of arable and gravel soil, and the underneath layer is dolomite with the sliding surface having an argillaceous interlayer. Manual removal of failed rock masses exposed an approximately 266-m-long smooth sliding surface with white and gray colored dolomite. The trailing edge of the 2014 rockslide produced a free surface with a vertical height of about 25 m (Fig. 4d, e), which became one of the sources for the 17 February 2019 rockslide.

There was no further deformation observed from the images after August 2016, even after a period of heavy rainfall in 2017. The slope was experiencing creep deformation within or below the surface rock mass. Since June 2018, a tensile crack with a width of 0.2 to 0.9 m was observed at the rockslide crown and it developed into a major discontinuity having a length of about 200 m, a width of 0.8 to 3.0 m and a depth of 33 m by 5 December 2018 (see Fig. 5). These were in situ visual observations which showed the signs of accelerated deformation, indicating the slope was marching into an unstable status. The major discontinuity developed since June 2018 can be seen from Fig. 4e. In addition, as shown in Fig. 4e, a small rock mass with a volume of about 20,000 m³ was collapsed on the northwest

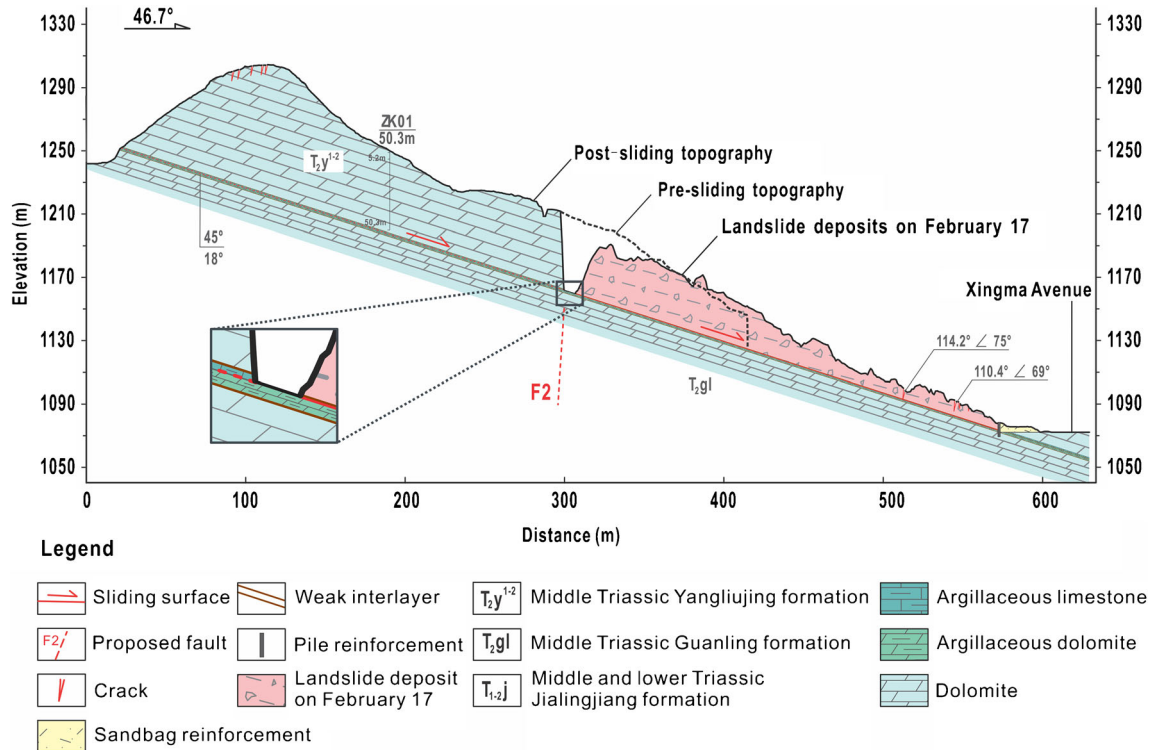


Fig. 3 Longitudinal profile taken along line 1–1' (Fig. 2) of the rockslide after 17 February 2019

side on 21 January 2019. The latest and large rockslide occurred at 5:53 a.m. on 17 February 2019, whose boundary is shown in Fig. 4f. This new failure was at the scarp and the sliding surface of the previous rockslide. Figure 4f also shows the highly deformed area affected by the first rockslide, where intensive cracks were developed in Zones I and II and eventually, these zones were found to be potentially unstable after the 17 February 2019 event.

Real-time landslide early warning system

Monitoring strategies

For the early warning of slow-moving/creep landslides, displacement and other displacement-derived quantities are the main monitoring parameters widely used all over the world (Pecoraro et al. 2018; Intrieri et al. 2019). For rockslides and rock falls, Pecoraro et al. (2018) review 6 landslide early warning systems, which use displacement and its derivatives (velocity and acceleration) as primary alert parameters measured by geotechnical, geodetic, and remote sensing techniques. Even though not all the in situ-monitored parameters are directly taken to define the alert criterion, they provide complementary information on landslide activity and additional updates for the LEWS.

In this study, we adopted a combined monitoring strategy with the use of geotechnical and geodetic methods. The deployment of the various sensors and its distribution on the site are illustrated in Fig. 6. Geotechnical monitoring was done by the crack gauges assessing direct measurements of ground displacements and a tiltmeter measuring tilt angle. Anyhow, the tiltmeter measurement was not used for the early warning as it was judged that displacement would be a better candidate to forecast the rockslide.

Geotechnical monitoring method is easy to implement and provides reliable data due to its simplicity and robustness. Meanwhile, the geodetic method by Global Navigation Satellite System (GNSS) identifies displacement by measuring distances tracked by Global Positioning System (GPS) satellite signals. Further, a rain gauge was installed to measure precipitation that may likely trigger a failure. Even though precipitation is not strictly considered as an alarm parameter or warning threshold for this rockslide, it may still promote the mechanical deterioration of the weak interlayer, which consists of argillaceous limestone and argillaceous dolomite. Nevertheless, no heavy rainfall is recorded before the 17 February 2019 rockslide, and it is clear that precipitation was not a crucial trigger that led to the sliding. Therefore, the installations of multiple types of monitoring sensors provide complementary information about the landslide activity and help to detect the spatial-temporal evolution of landslide for a reliable prediction, though not all of them are taken forward to the early warning system (Dunncliff and Green 1988). It is worth to point out that more than one monitoring method for ground displacements was employed to have alternatives in case of device malfunctioning due to weather and related disturbances and to keep the LEWS active during emergency scenarios.

Among these different sensors, the cumulative displacement obtained from crack gauges present the most continuous and reliable data during the accelerated deformation stage (Fig. 7). It is very important to capture the crucial information of displacement during imminent sliding, and in this aspect, crack gauges were preferred and its monitoring data was taken over to the LEWS instead of other displacement-based monitoring devices, i.e., GNSS. The displacement measurements from the crack gauges



Fig. 4 Visual interpretation of historical deformation of the rockslide from Google Earth images (the date is shown using YYYY/MM/DD format), **a** 2014/02/16, **b** 2014/11/27, **c** 2016/08/01, **d** 2017/11/16, **e** 2019/01/21, and **f** 2019/02/17. The numbers (1), (2), (3), (4), (5), and (6) in (e) are locations of photographs (see Fig. 5) taken along the orange scarp line

are shown in Fig. 7. A continuous progressive failure has been observed from the data. The inset inside Fig. 7 shows the progressive increase in rockmass displacement few hours before the failure.

A comparison between the crack gauges and GNSS sensors is shown in Fig. 8. In Fig. 8a, b, the data obtained from GNSS show an overall increased cumulative displacement trend than that of crack gauge and has a loss of data because of its fixed low-frequency sampling. With the advantage of a self-adaptive data acquisition technique developed by SKLGP (Zhu et al. 2017), the crack gauge can automatically adjust the sampling frequency with respect to the displacement rate (velocity). The crack-gauge sensor is designed to take samples at different frequencies, i.e., for the primary creep with a constant rate of deformation; the frequency is set relatively low in order to minimize energy consumption and while the rock mass is undergoing accelerated deformation, the sensor adjusts into high-frequency sampling to ensure high quality of data which is crucial in calculating displacement and other derived parameters.

Though newly developed instruments are adapted for monitoring, it does not mean the results will exactly fit the ideal curve of the three deformation phases (initial, constant, and accumulative) of creep slope failure (Saito 1969; Fukuzono 1985; Hao et al. 2016; Loew et al. 2016; Carlà et al. 2017; Intrieri et al. 2019). The deformation curve obtained from the monitoring device is inevitably influenced by a variety of external factors, i.e., noises arising due to nearby anthropogenic activities (for example activities near the road towards left of the rockslide in Fig. 6). For the processing of displacement monitoring data in our LEWS, the least squares method and moving average method are generally used for fitting and smoothening the original data (Qi 2017). The first method has the most important application in data fitting, which minimizes the sum of the squared difference between the observed value and fitted value (see Fig. 8b). When the rock mass is in a long period of “silence” or constant deformation stage, the least squares method is carried out for regression fitting. However, the slope deformation usually experiences a sudden acceleration when it enters a



Fig. 5 Enlarged view of discontinuities and cracks found along the landslide scarp (orange line in Fig. 4e) before the 17 February 2019 rockslide. Yellow dotted lines show the cracks surrounded by vegetation

highly accelerated state according to creep theory (Loew et al. 2016). At this stage, the crucial information for issuing alert messages will be deleted by the least squares method and hence the moving average method is introduced to overcome this limitation. When the displacement had increased significantly, the moving average method filters the noise, but highlights the trend of the displacement-time curve and keeps the complete data detected from sudden changes. It is important to automatically select the appropriate method to process monitoring data according to the characteristics of the displacement curve. In Fig. 8b, it can be seen that the least squares method is not appropriate for GNSS data since the slope has already undergone accelerated deformation. Our LEWS automatically calculates the rate increment, identifies the status of landslide deformation, and then selects the appropriate data processing method which we consider to be most advantageous during a critical emergency.

Multiple threshold method applied in the early warning system

In addition to the self-developed monitoring instruments and improved data processing methods, the final success of a LEWS relies exclusively on a precise warning model to determine

warning thresholds. The warning model defines a set of decision-making procedures required to issue an alert by including the determination of alert parameters, alert criteria, number of alert levels and warning message dissemination (Pecoraro et al. 2018). Many LEWS for rockslides employ correlation laws derived from statistical analyses of observed data from historical landslides in similar geological setting (Pecoraro et al. 2018). Based on the assumption of creep theory (Tavenas and Leroueil 1981), many researchers conducted empirical methods to extrapolate the time of failure through geometrical arguments (Intrieri et al. 2019). Specifically, they derive the relationships from the displacement-time curve to fit the typical creep curve and then calculate the inverse velocity from the fitted creep curve to estimate the failure time, when the velocity is theoretically infinite and inverse velocity approaches zero. The prediction of failure time is very important to issue precise alerts but unfortunately, it is still under theoretical research and successful application of the concept to a LEWS is even more limited.

The authors of this paper developed a general and quantitative criterion for LEWS (Xu et al. 2011). The criterion describes the tangential angle (α) referring to the deformation rate of the

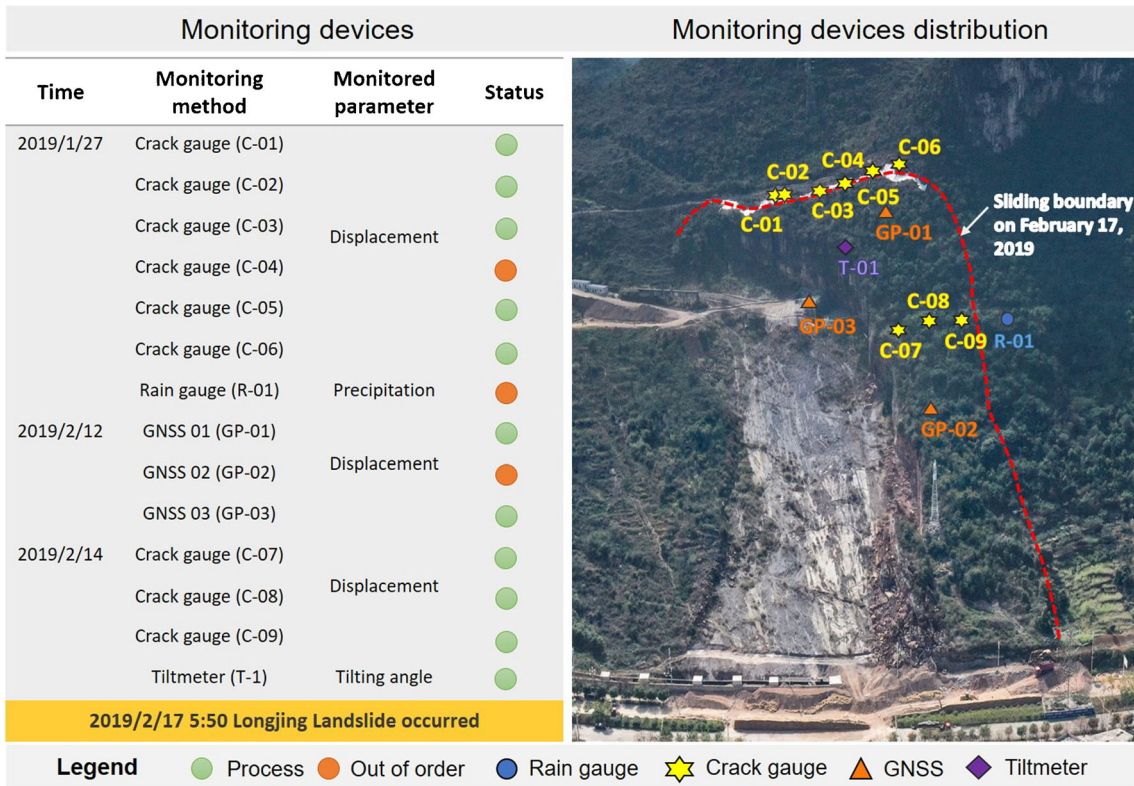


Fig. 6 Location and distribution of installed monitoring instruments

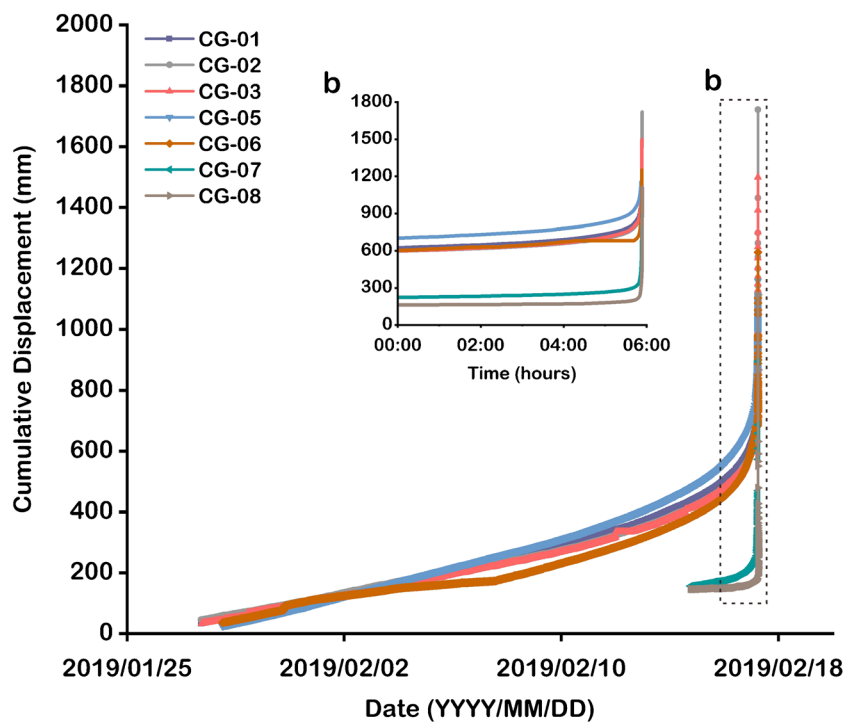


Fig. 7 Displacement measurements from different crack gauges

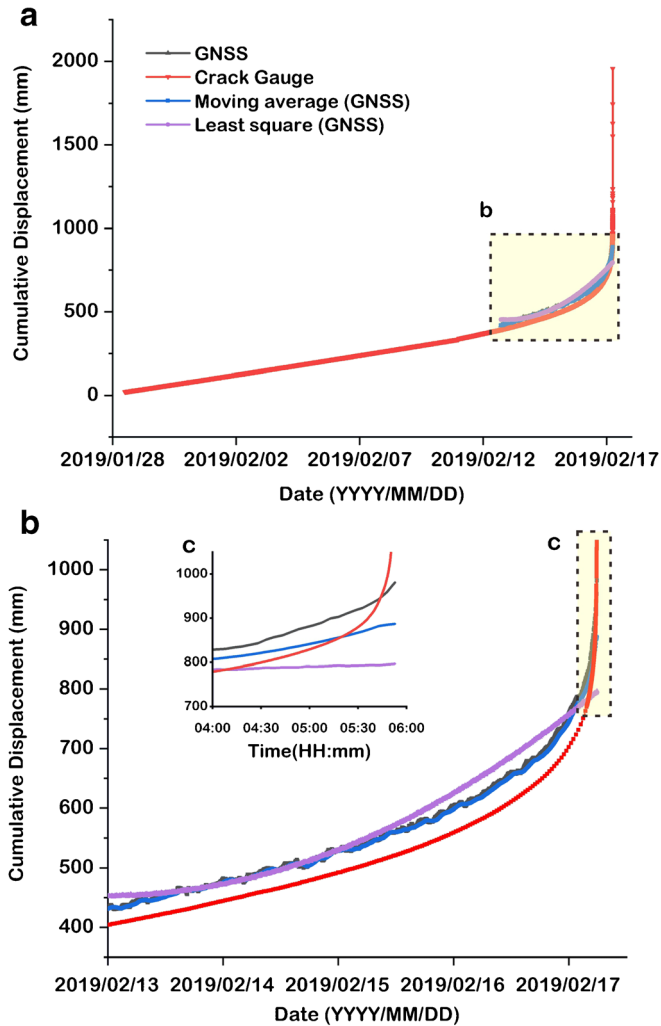


Fig. 8 Comparison and analysis of different filtering methods for data obtained from crack gauges and GNSS at Longjing **a** whole data and **b** enlarged portion **b** (the enlarged portion **c** shows the difference in data few hours before failure)

displacement-time curve at a given time and is used to specify different alert levels. Wang (1999) concluded that the value of α before imminent failure is generally 89° to 89.5° based on back analyses of a considerable number of landslides. Their finding proves that similarity of tangential angle exists among different landslides. This tangential angle method was verified using nine numbers of landslides with different failure mechanisms including rockslides (Xu et al. 2009, 2011) and loess landslides (Qi 2017; Qi et al. 2018). Altogether we analyzed deformation trends of more than 100 numbers of landslides, and out of those, details of 62 loess landslides are described in Peng et al. (2018). These back analyses of more than 100 landslides help to divide the accelerated phase into three sub-phases as illustrated in Fig. 9, which also shows the details of the warning model in our LEWS. Compared with the traditional thresholds of displacement and velocity, the thresholds of the tangential angle can be used for various types of landslides (see Sect. **Early warning and emergency mitigation measures**).

Though the tangential angle method is unique and advantageous, defining a single threshold based on it for all landslides will not be sufficient to make an accurate judgment on the trend of the

entire evolution process of landslide deformation. Due to this reason, multiple alert thresholds are established in our LEWS. On the basis of the tangential angle method, the incremental rate of deformation named as rate increment (Δv) measured in mm/timestep is used to identify the accelerated phases of deformation. The rate increment (Δv) does not differ much and assumed to be around 0 in the constant deformation phase. At the beginning of accelerated deformation, the rate increment (Δv) is mostly positive, but still fluctuates and its amplitude is larger than that of the constant deformation phase. The rapid growth of Δv usually indicates the premise of a failure. Different landslides exhibit different rate increments (Δv) and different deformation phase changes. For example, the loess landslides exhibit different rate increment (Δv) in the accelerated deformation phase and its amplitude varies more frequently within a very short span of time. In this case, the lead time would become very short to judge (see Sect. **Discussion** for more discussion on lead time). Moreover, there is still the possibility of missing or misjudging the alert using the tangential angle method. In that case, the velocity thresholds (v) based on statistical analyses derived from monitoring data of landslides occurred in the past play a vital role in further distinguishing the true deformation of landslides from equipment errors. As shown in Fig. 9, V_1 mainly identifies the state when the landslide begins to deform abnormally, while V_2 indicates whether the abnormal deformation of the landslide enters a relatively fast degree. V_3 determines whether the deformation exceeds the short-time rapid deformation of the landslide caused by most possibly a new crack. The multiple threshold method makes our early warning system effective.

Early warning and emergency mitigation measures

For the case of Longjing rockslide, we lack monitoring data of early deformations or similar landslides of this kind to extract and define velocity thresholds. Thus, only tangential angle (α) and rate increment (Δv) thresholds were considered alert parameters in the LEWS. The displacement-time curves collected by crack gauges and GNSS are used to get the real-time value of α and Δv . Considering the quality of data (discussed previously in Sect. **Monitoring strategies**), the crack gauge performs better than GNSS with higher accuracy for determining the thresholds. After the installation of the monitoring network on site in January 2019, our LEWS can receive real-time data transmitted from the field and automatically calculate the α for each crack gauge in parallel. An alert message will be issued respectively considering the deformation development from each sensor. Figure 10a shows the cumulative displacement after data processing as obtained by crack gauge C-05, which firstly sent the warning message of imminent sliding at 5:00 a.m., 17 February 2019.

The curves of velocity (v), tangential angle (α), and rate increment (Δv) were derived as shown in Fig. 10a. Xu et al. (2011) highlight the importance of fixing the time interval, determining the deformation rate, and the method for calculating the α (Fig. 9) starting from the initial deformation phase. However, in our case, it is worth to note that the slope has already reached the phase of constant deformation when devices were set up and hence the LEWS straightaway started analyzing the real-time data and issued the alert level as discussed in Sect. **Background**.

Emergency mitigation measures were initiated in early January 2019. A chronology of the mitigation measures performed is

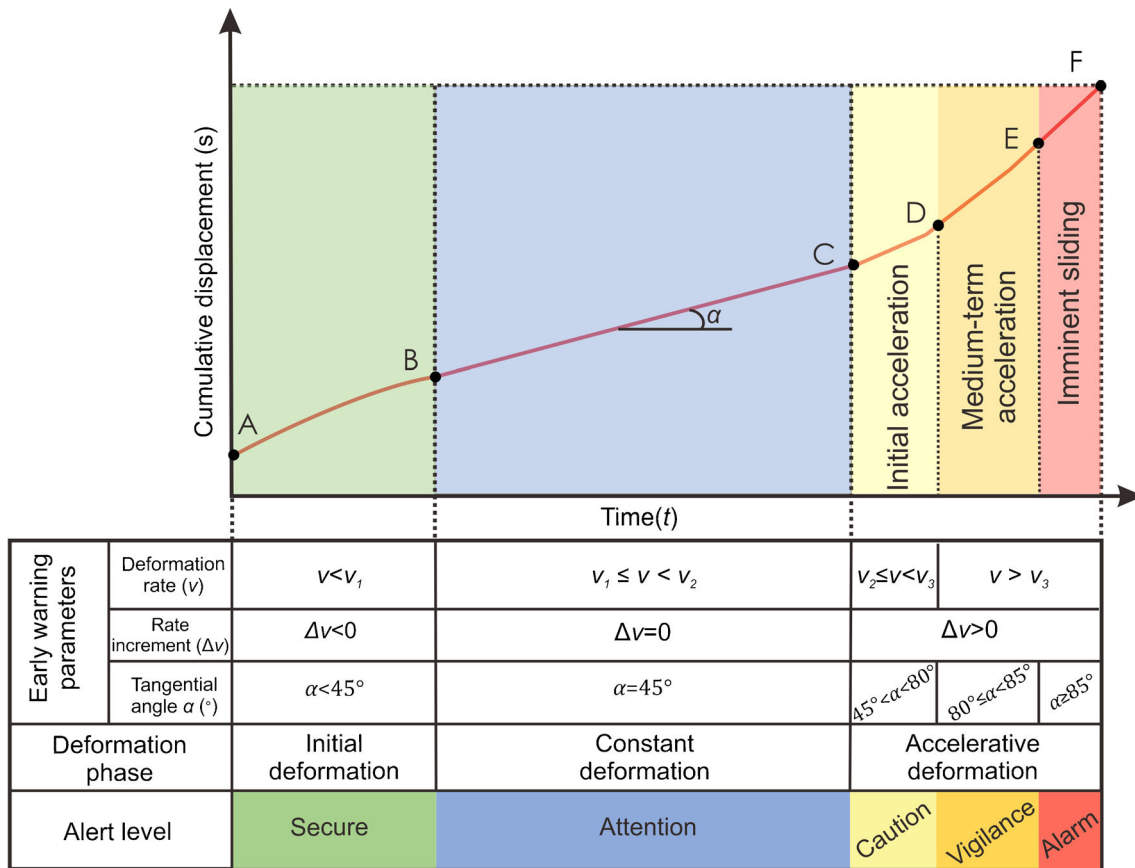


Fig. 9 Concept of warning criteria of the landslide early warning system developed by SKLGP

summarized in Table 1 and only the most significant events are described in the following. The emergency response was launched on 7 January 2019. The following mitigation measures, including anti-slide pile reinforcements at the rockslide toe and stacking sandbags at the back scarp, was carried out step by step. During the construction, on 21 January 2019, a small collapse happened at the left front edge of the slope. It buried two of the reinforcement piles with a volume of around 20,000 m³ but fortunately, there were no casualties or injuries. Since further collapses were suspected, additional sandbags were stacked at the slope toe to reduce the runout of rock masses in case of a large failure. The LEWS was installed on the slope on 27 January 2019. Just 2 days later on 29 January, the cracks at the rockslide crown were begun developing with a deformation rate of around 20 mm/day. In response to this threat, based on an instruction from the LEWS team, the local government evacuated over 400 people who were living on the premises around the highway.

The LEWS automatically broadcasted “Caution” (italicized) on 15 February 2019, as the value of α was more than 45°, which also means the rockslide entered accelerative deformation phase. Based on our suggestion, on 15 February 2019, prompt action was taken by the local government closing the access to the road and preventing public interference in the near vicinity. The very next day, the values of v , Δv , and α increased significantly. Before the α reached 80° with a warning message of “Vigilance” in bold, all the personnel and equipment on site performing structural mitigation

measures were evacuated. At 5:00 am on 17 February 2019, the system sent a warning message in alarm level (bold-italic) with a deformation rate exceeding 251 mm/day, cumulative displacement of 829.2 mm and a tangential angle above 85°, explicating very high possibility of failure in a short period of time. Warnings were first sent to the Emergency Response Center of Guizhou Province and then forwarded to the local government and residents through short message service (SMS) messages and smartphone APP. The previous alert messages until 17 February 2019, were announced as internal statements only to politicians, government institutions, and technical experts. Only the final alarm of imminent sliding was sent to the public as an SMS in order to avoid unnecessary panic. Above all, the LEWS successfully warned the occurrence of rockslide and played a vital role in emergency response. Since more frequent rock mass failures are expected in the future, currently the LEWS continues to monitor the case. Meanwhile, additional mitigation measures and reconstruction of the affected site are underway whose details are planned to be presented in a future research article.

Discussion

Many studies report the observed displacement time series following the three-phase slope creep curve for an early warning model, which is regarded as a significant part of the LEWS (Fukozono 1990; Crosta and Agliardi 2003; Ju et al. 2015; Loew et al. 2016; Intrieri et al. 2019). Saito (1965) indicated that the slope creep

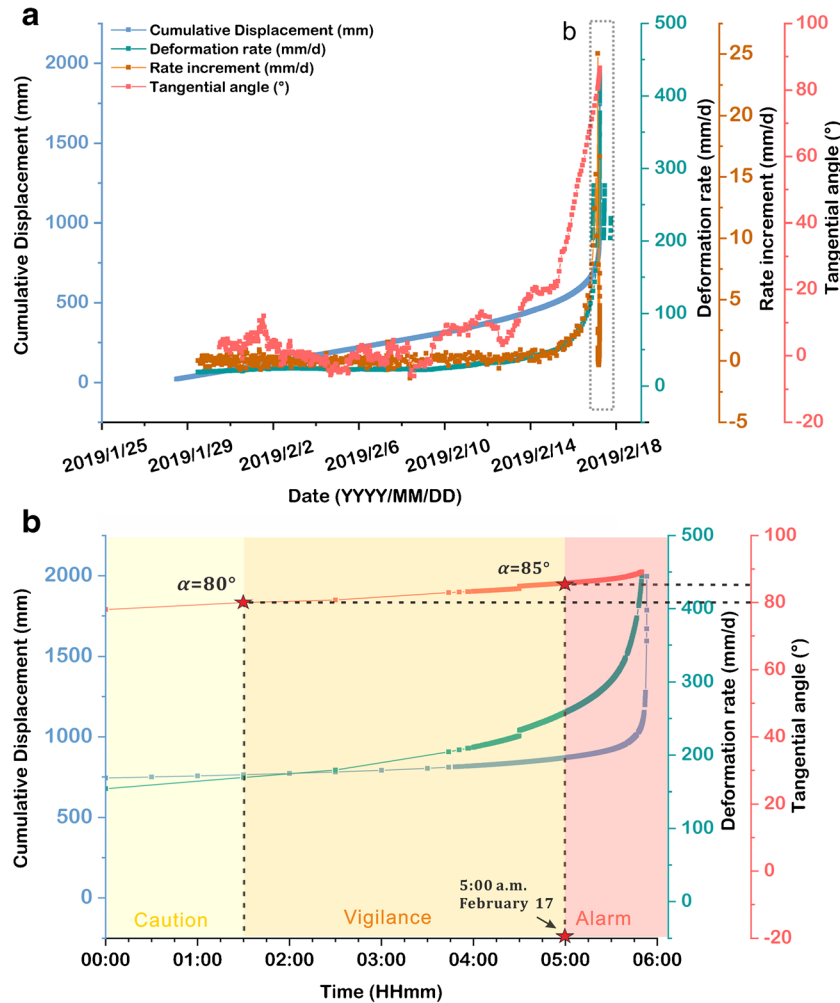


Fig. 10 Cumulative displacement obtained by crack gauge C-05 and the derived curves of α , v , and Δv with corresponding alert levels a data from 27 January 2019 to 17 February 2019 and b data few hours before the failure

usually showed a non-linear time-displacement relationship and prompted a sudden increase in the deformation rate before complete failure. Based on the slope creep theory, many empirical methods were adopted to forecast the time of slope failure (Saito 1969). Fukuzono (1985) and Voight (1988) derived a time-dependent relationship and developed a power-law function between failure time and displacement velocity, which was more physically based on the method developed by Saito (1969). The model was further improved by Crosta and Agliardi (2003) through introducing controlling parameters into the velocity curve, assuming these parameters were representative of the mechanical behavior of the rock approaching failure. Similarly, Loew et al. (2016) applied an S-shape curve to fit the monitored time-displacement curve, which was based on a relatively simple mathematical equation which describes the fatigue failure and deformation of rock (Xiao et al. 2009). Meanwhile, velocity thresholds were proposed for different alert levels, which are frequently used in most LEWS. However, most velocity thresholds are determined by an observational approach through back analysis of other previous landslides in a similar geological setting. The velocities are different from one specific site to another, and even within a

single landslide, the deformation rate prior to the failure changes considerably from a few millimeters per day to meters per day. These make it rather difficult to obtain or determine the velocity thresholds for early warning.

To overcome the above-mentioned constraints, our previous research investigated the tangential angle of the displacement-time curve as well as the acceleration characteristics during slope deformation (Xu et al. 2009, 2011). A new warning criterion based on the tangential angle was proposed and applied in our LEWS (Huang et al. 2012b, 2015; Ju et al. 2015), which successfully predicted the disastrous rockslide presented in this study (see Sect. [Early warning and emergency mitigation measures](#)). In addition, our LEWS also successfully predicted loess landslides at four more occasions in Heifangtai Terrace, Gansu province, China between 2017 and 2019 (Huan 2017; He 2019; Petley 2019). Along with the thresholds of tangential angle, multi-level velocities (see Sect. [Background](#)) are also defined to improve the accuracy of LEWS. Our LEWS has been validated and proved to be effective to predict at least two types of landslides, i.e., rockslides and shallow soil slides so far due to its consideration of different and multiple-level thresholds. Hereby, we recommend adopting different and multiple-levels of thresholds, i.e.,

Table 1 Chronology of mitigation measures applied and associated warning messages

Timescale	Mitigation measures
7 Jan 2019	The emergency response was launched.
8 Jan 2019	Construction of anti-slide pile reinforcement with retaining wall at the rockslide toe was started. The concrete pouring of 7 anti-slide piles was finished before 17th February 2019.
16 Jan 2019	Sandbags were stacked at the scarp of rockslide with an approximate volume of 10,000 m ³ . At Zone, I, the anchor rods with concrete support was under construction.
21 Jan 2019	A collapse occurred at the left front edge of the rockslide with a volume of around 20,000 m ³ . All personnel in the dangerous area were evacuated quickly.
22 Jan 2019	Additional sandbags were stacked to build a wall at the left front of the Xingma Avenue. Shielding of tensile cracks and drainage ditch construction started.
27 Jan 2019	As invited by the Department of Natural Resources, Guizhou Province, the monitoring network was installed on-site, including 6 self-adaptive crack gauges and a rain gauge.
29 Jan 2019	400 residents were evacuated as the deformation rate exceeded 20 mm/day.
12 Feb 2019	Three GNSS sensors were installed.
13 Feb 2019	Other anti-slide pile reinforcements were under construction at the left front edge of the landslide. Pouring of concrete was finished for 6 piles.
14 Feb 2019	3 additional crack gauges were installed.
15 Feb 2019	<i>The alert level of “Caution” was issued by the LEWS.</i> Access to the danger zones around the rockslide was barred to prevent public interference in the near vicinity.
16 Feb 2019	The alert level of “Vigilance” was issued by the LEWS. Construction workers, engineers, and related equipment were evacuated.
At 5:00 a.m., 17 Feb 2019	The alert level of “Alarm” was issued by the LEWS, which indicated the imminent sliding. Information sent out to the public by SMS messages, and relevant departments were informed to prepare additional disaster prevention measures.
At 5:53 a.m., 17 Feb 2019	The rockslide occurred.

displacement (mm), rate of displacement/velocity (mm/per time step), incremental velocity and tangential angle (°), etc. together in a LEWS in order to improve its preciseness and extend its applicability for different types of landslides.

Our experiences also complement the advantages of using multiple monitoring strategies in a LEWS. In the case of Longjing rockslide and other loess landslides, it was found that usage of different types of monitoring methods through various kinds of sensors, i.e., crack gauges, GNSS, etc. were helpful in determining which one(s) should be taken forward to the LEWS to issue the final alert. As we discussed earlier in Sect. [Monitoring strategies](#), we found the crack gauges are most suitable in our case to accurately predict the deformation behavior, though usage of other sensors in parallel will always add an advantage. The self-

adaptive data acquisition technique also adds another advantage to the crack gauges. It is also important to select the right crack gauge to issue the alert even though all the crack gauges were monitored simultaneously. Based on our experience, we selected the group of devices whichever reached a tangential angle of 45°, 80°, and 85° consecutively at the earliest.

The detection and forecast of landslides well advance in time by the LEWS is much essential to facilitate the evacuation process (Sättele et al. 2012; Stähli et al. 2015). We compared the lead time from all the five successful cases of the early warning done by the LEWS (Table 2). The first four cases are loess landslides and the final one is the recent Longjing rockslide. In the first case, the LEWS forecasted the landslide approximately an hour before, the alert message was sent out exactly after 22 min, and finally, the

Table 2 Comparison of lead time from all the successful landslide predictions by the LEWS

Landslide	Imminent sliding alert (LEWS $\alpha > 85^\circ$)	Alert message conveyance (expert's decision)	The actual occurrence of landslide	Lead time (h)
Chengjia—1 (Heifangtai, Gansu)	13 May 2017 (8:51)	13 May 2017 (9:13)	13 May 2017 (9:52)	1.02
Dangchuan—1 (Heifangtai, Gansu)	30 Sep 2017 (17:50)	30 Sep 2017 (20:55)	1 Oct 2017 (5:00)	11.17
Chengjia—2 (Heifangtai, Gansu)	3 Mar 2019 (22:18)	3 Mar 2019 (23:17)	4 Mar 2019 (0:19)	1.03
Dangchuan—2 (Heifangtai, Gansu)	26 Mar 2019 (4:20)	26 Mar 2019 (4:34)	26 Mar 2019 (5:01)	0.68
Longjing (Xingyi, Guizhou)	17 Feb 2019 (5:00)	17 Feb 2019 (5:00)	17 Feb 2019 (5:53)	0.88

actual occurrence timed 1 h later. The other three cases of loess landslides also have these timings as can be seen from Table 2. For the Longjing case, the forecast was done less than an hour before the actual rockslide and the expert decision on sending the alert message was done at once at the same time. Whereas for all the other four cases, the expert suggestion came at least 14 min later than the alert from the LEWS (the second case came after 3 h). This time difference states that though we have an advanced LEWS, it still needs to be double confirmed by scientists to decide whether or not to send an alert message to the public in order to avoid false alarms.

Conclusions

The cases of successful prediction and mitigation of landslides are very exceptional worldwide due to their complex nature. Early warning systems are valuable tools for risk reduction, and they empower the community by providing timely alerts spanning hours, thus saving invaluable lives. In this study, we presented a successful case of early warning and emergency mitigation measures accomplished for a disastrous rockslide in Southwestern China. Our self-developed LEWS helped to predict and mitigate the rockslide, eventually achieving zero casualties or injuries and almost no property losses. We also discussed the other four landslides that were successfully predicted by our LEWS. The improved data processing method and the early warning model based on multiple threshold determination methods were introduced. Our study also contributes to the compilation of a comprehensive database of displacement time histories of landslides that will be helpful for predicting similar landslides in the future. The experiences we have learned from the successful cases are summarized as follows:

- The Longjing rockslide was initially triggered by anthropogenic activities and with time developed into a major disaster needing special attention and exclusive mitigation measures. Since the initial trigger is a manmade slope excavation, this experience also brings out the consequences of underestimating the role of hillslope geology. It is very clear that no prior investigation in 2014 was done regarding the hill slope stability under the influence of the amount of rock mass removed from the slope toe. The necessity of performing a thorough geotechnical stability investigation of adjacent hillslopes along transport network has clearly been understood.
- Satellite images are very helpful to track the deformation history of landslides especially for cases where deformation is ongoing and there is a lack of continuous monitoring data. For the Longjing rockslide, it is with the help of initial interpretation from freely available satellite images; the mitigation measures have been planned and carried out.
- Knowledge of site conditions play an imminent role before, during, and after setting up the LEWS and both the in situ monitoring and mitigation measures should be carried out simultaneously to prevent minor to major disasters in quick time.
- The importance of considering different and multiple-level thresholds (criteria) in an early warning system is substantially proven. We recommend the use of multiple thresholds measured from different sensors together to keep the system uninterrupted and reliable during an emergency.

Acknowledgments

We would like to thank the contribution of the governmental staffs from Guizhou province, Mr. Caizhong Xiao, Mr. Xiuwei Liu, Mr. Guoxuan Zhao, and many other experts who were involved in the early warning and emergency mitigation.

Funding information

This study is funded by the National Science Fund for Outstanding Young Scholars of China (Grant No. 41622206), the Fund for Creative Research Groups of China (Grant No. 41521002), and the National Key R&D Program of China (No. 2017YFC1501002).

References

- Carlà T, Farina P, Intrieri E, Botsialas K, Casagli N (2017) On the monitoring and early-warning of brittle slope failures in hard rock masses: examples from an open-pit mine. *Eng Geol* 228:71–81. <https://doi.org/10.1016/j.enggeo.2017.08.007>
- Crosta GB, Agliardi F (2003) Failure forecast for large rock slides by surface displacement measurements. *Can Geotech J* 40:176–191. <https://doi.org/10.1139/t02-085>
- Dunnicliff J, Green GE (1988) *Geotechnical instrumentation for monitoring field performance*. Wiley-Interscience, New York
- Fan X, Xu Q, Alonso-Rodriguez A, Siva Subramanian S, Li W, Zheng G, Dong X, Huang R (2019) Successive landsliding and damming of the jinsha river in eastern tibet, china: Prime investigation, early warning, and emergency response. *Landslides* 16:1003–1020. <https://doi.org/10.1007/s10346-019-01159-x>
- Fukuzono T (1990) Recent studies on time prediction of slope failure. *Landslide News* 4:9–12
- Fukuzono T (1985) A new method for predicting the failure time of a slope. 4th international conference and field workshop on landslide. Tokyo University Press, Tokyo, pp 145–150
- Gariano SL, Guzzetti F (2016) Landslides in a changing climate. *Earth Sci Rev* 162:227–252. <https://doi.org/10.1016/j.earscirev.2016.08.011>
- Guo F, Jiang G, Yuan D, Polk JS (2013) Evolution of major environmental geological problems in karst areas of southwestern china. *Environ Earth Sci* 69:2427–2435. <https://doi.org/10.1007/s12665-012-2070-8>
- Hao S, Liu C, Lu C, Elsworth D (2016) A relation to predict the failure of materials and potential application to volcanic eruptions and landslides, vol 6, p 27877. <https://doi.org/10.1038/srep27877>
- He S (2019) Chinese researchers successfully predicted Longjing landslide, Xingyi, Guizhou China News (in Chinese)
- Huan X (2017) Alarm the landslide 9 hours in advance from thousands miles. *Chengdu Commercial Daily*, Chengdu (in Chinese)
- Huang M, Qi S, Shang G (2012a) Karst landslides hazard during 1940–2002 in the mountainous region of guizhou province, southwest china. *Nat Hazards* 60:781–784. <https://doi.org/10.1007/s11069-011-0018-z>
- Huang R, Huang J, Ju N, He C, Li W (2012b) Webgis-based information management system for landslides triggered by wenchuan earthquake. *Nat Hazards* 65:1507–1517. <https://doi.org/10.1007/s11069-012-0424-x>
- Huang J, Huang R, Ju N, Xu Q, He C (2015) 3d webgis-based platform for debris flow early warning: aq case study. *Eng Geol* 197:57–66. <https://doi.org/10.1016/j.enggeo.2015.08.013>
- Intrieri E, Carlà T, Gigli G (2019) Forecasting the time of failure of landslides at slope-scale: a literature review. *Earth Sci Rev* 193:333–349. <https://doi.org/10.1016/j.earscirev.2019.03.019>
- Ju N, Huang J, Huang R, He C, Li Y (2015) A real-time monitoring and early warning system for landslides in southwest china. *J Mountain Sci* 12:1219–1228. <https://doi.org/10.1007/s11629-014-3307-7>
- Loew S, Gschwind S, Gisich V, Keller-Signer A, Valenti G (2016) Monitoring and early warning of the 2012 preonzo catastrophic rockslope failure. *Landslides* 14:141–154. <https://doi.org/10.1007/s10346-016-0701-y>
- Pecoraro G, Calvello M, Picillo L (2018) Monitoring strategies for local landslide early warning systems. *Landslides* 16:213–231. <https://doi.org/10.1007/s10346-018-1068-z>
- Peng D, Xu Q, Liu F, He Y, Zhang S, Qi X, Zhao K, Zhang X (2018) Distribution and failure modes of the landslides in heitai terrace, china. *Eng Geol* 236:97–110. <https://doi.org/10.1016/j.enggeo.2017.09.016>

- Petley D (2019) Longjing village: Successful prediction of a significant rockslide. The Landslide Blog. <https://blogs.agu.org/landslideblog/2019/02/22/longjing-village-landslide/> date accessed: 24 Apr 2019
- Popescu ME, Sasahara K (2009) Engineering measures for landslide disaster mitigation. In: Sassa K, Canuti P (eds) Landslides—disaster risk reduction. Springer, Berlin, pp 609–631
- Qi X (2017) Sudden loess landslide monitoring and early warning research—a case study of Gansu landslide in Heifangtai loess. Chengdu Univ Technol, Chengdu (in Chinese)
- Qi X, Xu Q, Liu F (2018) Analysis of retrogressive loess flowslides in heifangtai, china. Eng Geol 236:119–128. <https://doi.org/10.1016/j.enggeo.2017.08.028>
- Saito M (1965) Forecasting the time of occurrence of a slope failure. In: Proceedings of 6th international conference on soil mechanics and foundation engineering. University of Toronto Press, Montreal, pp 537–541
- Saito M (1969) Forecasting time of slope failure by tertiary creep. In: Proceedings of 7th international conference on soil mechanics and foundation engineering, Mexico, pp 677–683
- Sättele M, Bründl M, Straub D (2012) A classification of warning system for natural hazards. 10th international probabilistic workshop, Stuttgart, pp 257–270
- Stähli M, Sättele M, Huggel C, McArdell BW, Lehmann P, Van Herwijnen A, Berne A, Schleiss M, Ferrari A, Kos A, Or D and Springman SM (2015) Monitoring and prediction in early warning systems for rapid mass movements. Nat Hazards Earth Syst Sci 15: 905–917. doi: <https://doi.org/10.5194/nhess-15-905-2015>
- Tavenas F, Leroueil S (1981) Creep and failure of slopes in clays. Can Geotech J 18:106–120. <https://doi.org/10.1139/t81-010>
- Voight B (1988) A method for prediction of volcanic eruptions. Nature 332:125–130. <https://doi.org/10.1038/332125a0>
- Wang J (1999) Study on engineering geology of typical high-stepped loess landslide group. Chengdu Univ Technol, Chengdu (in Chinese)
- Xiao J-Q, Ding D-X, Xu G, Jiang F-L (2009) Inverted s-shaped model for nonlinear fatigue damage of rock. Int J Rock Mech Min Sci 46:643–648. <https://doi.org/10.1016/j.ijrmms.2008.11.002>
- Xu Q, Zeng Y, Qian J, Wang C (2009) Study on a improved tangential angle and the corresponding landslide pre-warning criteria. Geol Bull China 28:501–505. [https://doi.org/10.1016/S1003-6326\(09\)60084-4](https://doi.org/10.1016/S1003-6326(09)60084-4)
- Xu Q, Yuan Y, Zeng Y, Hack R (2011) Some new pre-warning criteria for creep slope failure. Sci China Technol Sci 54:210–220. <https://doi.org/10.1007/s11431-011-4640-5>
- Zhu X, Xu Q, Qi X, Liu H (2017) A self-adaptive data acquisition technique and its application in landslide monitoring. Springer International Publishing, Cham, pp 71–78

Highlights

- Successful early warning and mitigation of a catastrophic reactivated rockslide with a total volume > 1 million m³ which occurred many years after the initial failure.
 - Evacuation information sent out hours before the failure saving more than 400 lives in the near vicinity. Casualties, injuries, and economic losses were successfully averted through quick and integrated action by scientists and local authorities.
 - We present the success story including the first report of site conditions, an overview of slope displacement, early warning, mitigation measures, and emergency response.

X. Fan · Q. Xu (✉) · **J. Liu** · **S. S. Subramanian** (✉) · **C. He** · **X. Zhu** · **L. Zhou**
 State Key Laboratory of Geohazard Prevention and Geoenvironment Protection,
 Chengdu University of Technology,
 Chengdu, Sichuan, China
 Email: xq-68@qq.com
 Email: srikrishnan@frontier.hokudai.ac.jp